Structural, Thermal, and Tribological Properties of Intercalated Polyoxymethylene/Molybdenum Disulfide Nanocomposites

J. Wang,[1] K. H. Hu,[2] Y. F. Xu,[2] X. G. Hu[2]

[1]*School of Chemical Engineering, Hefei University of Technology, Hefei 230009, China*
[2]*Institute of Tribology, Hefei University of Technology, Hefei 230009, China*

Received 12 July 2007; accepted 18 March 2008
DOI 10.1002/app.28519
Published online 13 June 2008 in Wiley InterScience (www.interscience.wiley.com).

ABSTRACT: Intercalated polyoxymethylene (POM)/molybdenum disulfide (MoS_2) nanocomposites were prepared by *in situ* intercalation/polymerization. The structures of the composites were characterized by means of powder X-ray diffraction (XRD) and transmission electron microscopy. The XRD pattern showed that the polymer was inserted into the MoS_2 galleries. The interlayer spacing of the intercalated phase increased from 6.15 to 11.18 Å. The thermal behavior of the composites was also investigated through thermogravimetric analysis. The results show that the heat resistance of the intercalated composites decreased slightly. The tribological behavior of POM/MoS_2 was investigated on an MQ-800 end-face tirbometer under dry friction. The worn surfaces were observed by scanning electron microscopy. The results show that POM/MoS_2 presented better friction reduction and wear resistance, especially under high load. The friction mechanism of the nanocomposites is also discussed in association with X-ray photoelectron spectroscopy. © 2008 Wiley Periodicals, Inc. J Appl Polym Sci 110: 91–96, 2008

Key words: inorganic materials; mechanical properties; nanocomposites; particle size distribution; thermal properties

INTRODUCTION

There has considerable interest and research activity in the preparation and characterization of layered nanostructured composites containing polymers.[1–4] Layered nanocomposites can improve mechanical and thermal properties, fire retardancy, electric conductivity, and so on. The intercalated technique provides a good method for resolving the dispersion of the material on a nanoscale range.

Transition metal dihalogenides (MX_2) have layered crystal structures, which have attracted significant attention over recent years.[5–9] Molybdenum disulfide (MoS_2) has great technological importance as catalysts (for the petrochemical hydrotreatment process), electrodes, solid-state lubricants, and materials with unusual two-dimensional magnetic properties.[10] As it was recently understood, the use of single-layer MoS_2 dispersions allowed an extension of the nature of guests.[11] Some polymer matrix nanocomposites with water solubility have been prepared by the exfoliation–adsorption technique.[5,6] The composites can be obtained quite easily by treatment of the product of the intercalation of lithium in MoS_2 with an aqueous solution of the polymer because the aqueous polymer is compatible with the single-layer water suspension of MoS_2.

In this study, the polyoxymethylene (POM)/MoS_2 nanocomposites were prepared by means of *in situ* intercalation/polymerization. POM is one kind of engineering plastic with self-lubrication properties. Some studies have involved modified POM with different solid lubricant additives for self-lubrication applications.[12–14] As a solid lubricant, MoS_2 is always blended with plastics directly. It is indeed hard to make the blend disperse uniformly for the sake of compatibility, and it would weaken the performances of polymer composites. In our previous research,[15] we confirmed that the mechanical and tribological properties of POM were better when the nanosized particles were dispersed into the POM matrix uniformly. However, it is possible to obtain a uniform blend on nanoscale via *in situ* intercalation/polymerization. It was reported that ultrasonication could help the intercalation.[16] In this experiment, ultrasonication technology was also used for assistance. The tribological performance was researched at high load values to provide some fundamental information for high-load applications, such as sliding bearing systems with higher loads.

Correspondence to: X. G. Hu (xghu@hfut.edu.cn).
Contract grant sponsor: National Natural Science Foundation of China; contract grant number: 50475071.
Contract grant sponsor: Anhui Provincial Natural Science Foundation; contract grant number: 070414152.

EXPERIMENTAL

Materials

Trioxane with chemical purity was purchased from Shanghai Chemical Factory (Shanghai, China) and was recrystallized in ethane dichloridize before use. Dioxolane with chemical purity was from Acros Orgaics Co., Ltd. Boron trifluoride etherate for use as a catalyst, hexahydrobenzene for use as a solvent, ethane dichloridize, and ammonia water were all purchased from National Reagent Corp. (Shanghai, China). They were further purified before use. MoS_2 and *n*-BuLi were purchased from Anhui Metallurgy Institute (Hefei, China) and Yangzhou Chemicals Co, (Yangzhou, China) respectively.

Preparation of the intercalated POM/MoS_2 composites

The preparation processing of restacked MoS_2 was performed as described in ref. 17. The cationic ring-opening copolymerization of the monomers trioxane and dioxolane (5.0 wt %) proceeded at 65°C in solution. A solution with two monomers was added to a dry, three-necked bottle under a nitrogen atmosphere, and then, the desired amount of restacked MoS_2 (2.0 wt %) was added to the solution. The mixture was stirred by a vortex and ultrasonicated for 30 min. Finally, the initiator was introduced into the flask. The reaction continued at 60°C for 2 h and was then treated in 5.0 wt % ammonia at 140°C for 5 h. The treated suspension was filtered, and the obtained residue was washed with deionized water and acetone several times. The obtained copolymers were dried *in vacuo*. Pure POM copolymer was also prepared as a comparative sample.

Characterization of the POM/MoS_2 nanocomposites

The lattice spacing of the composites was monitored on a Philips X'Pert Pro Super diffractometer with graphite-monochromatized Cu Kα radiation (Philips Co., Holland) (λ = 1.54178 Å). A JEM-100SX transmission electron microscope was used to observe the morphology of the POM/MoS_2 nanocomposites. A thermogravimetry/differential thermal analysis instrument (Shimadzu Co., Japan) was used to evaluate the thermal properties of the composite. Samples of about 5 mg were heated from ambient temperature to approximately 400°C at a rate of 10°C/min under an argon atmosphere.

Friction and wear tests were conducted with an MQ-800 end-face tribometer (Jinan, China) with AISI 1045 steel sliding against the polymeric composites with a face-contacting method in air (relative humidity = 75%) at room temperature (20°C) with a sliding velocity of 0.8 m/s under dry friction. The schematic diagram for the MQ-800 end-face tribometer is shown in Figure 1. The average surface roughness values of the steel and composite, determined from random surfaces (isotropic roughness texture) with central line average (CLA) surface roughness values, were 1.5 and 5.8 μm, respectively, after polishing. Their measurements were done by means of a Taylor–Hobson model 6 profilometer (Taylor-Hobson Co., UK). The morphologies of the wear scar were observed with a JSM-6700 field emission scanning electron microscope (Electron Co., Japan). The elements of the counterpart steel surface were investigated on VG model Escalab 250 X-ray photoelectron spectroscope (Thermo Electron, USA).

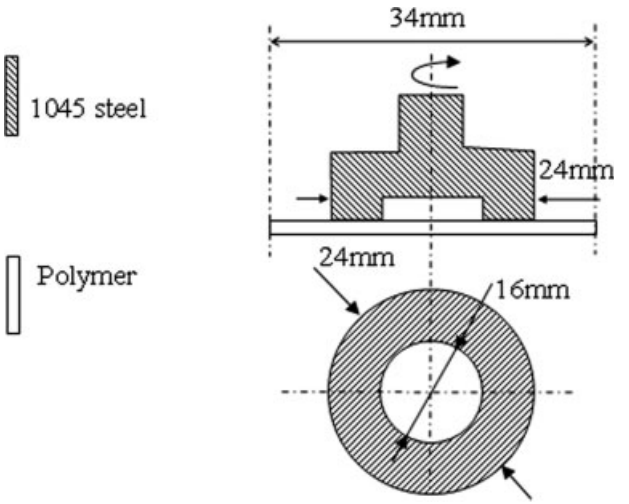

Figure 1 Schematic illustration of the end-face friction tribometer.

RESULTS AND DISCUSSION

Structure of the POM/MoS_2 nanocomposites

Figure 2 presents the XRD patterns of POM/MoS_2 and 2H-MoS_2 (tri-prism configuration). Figure 2(a) shows that the POM was crystalline. The feature diffraction peak (2θ = 23.06°) was ascribed to the 100 reflections of hexagonal POM.[18] XRD data also demonstrated that POM was intercalated into MoS_2. The first two (001) reflections were almost covered compared with the strong diffraction peaks of POM. The two reflections were observed clearly from the magnified drawing of the partial zone. In comparison with the 002 reflection at 2θ = 14.4° (*d*-spacing = 6.15 Å) of 2H-MoS_2 [Fig. 2(b)], the peak at about 8° (*d*-spacing = 11.18 Å) indicated that the spaces of the gallery were expanded, and the interlayer space expansion was 5.03 Å with respect to pristine MoS_2.

From the results of XRD, we deduced the intercalation mechanism of POM into MoS_2. In this cationic polymerization, when the nonpolar hexahydrobenzene was chosen for the solvent, the boron

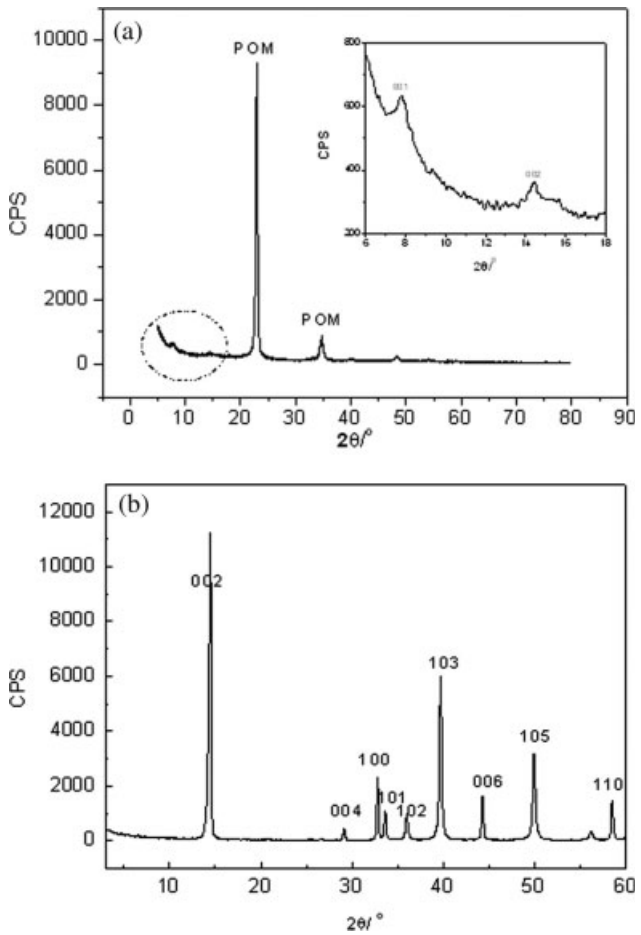

Figure 2 XRD patterns of (a) POM/MoS_2 and (b) 2H-MoS_2 (CPS = counts per second).

triflouride etherate acted as a catalyst, and water acted as the cocatalyst. The partly dissociated reaction of boron trifluoride etherate in hexahydrobenzene was as follows:

$$BF_3Et_2O + H_2O \rightleftharpoons BF_3OH_2 + Et_2O$$

$$BF_3OH_2 \rightleftharpoons H^+(BF_3OH)^-$$

It was an equilibrium reaction; the H^+ from the reaction could initiate the trioxane copolymerized with dioxolane. When the single-layer MoS_2 suspension was restacked, some water molecules were combined into the gallery of MoS_2 simultaneously. These co-intercalated water molecules participated in the reaction and acted as the cocatalyst. Thus, the monomers could insert into the galleries, and polymerization could also happen here.

Figure 3 represents the microscopy of the POM/MoS_2 nanocomposites. As shown, MoS_2 dispersed in the polymer matrix still had a layered structure, which was consistent with the XRD results mentioned previously. That is, the POM/MoS_2 composites were intercalated compounds, which was

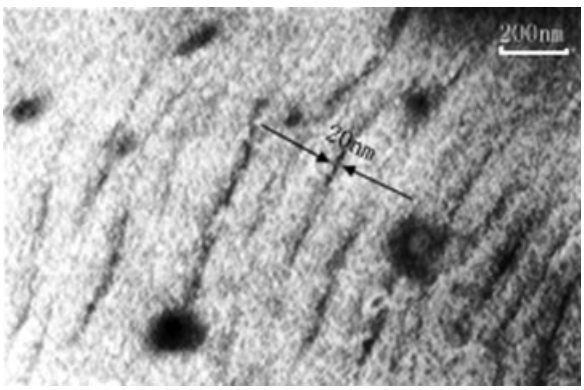

Figure 3 TEM image of the POM/MoS_2 nanocomposites.

important for the tribological performance of the POM/MoS_2 nanocomposites. The layered structure of MoS_2 is the basis of its use as a solid lubricant. The thickness of layered MoS_2 in the POM matrix was about 20 nm according to the transmission electron microscopy (TEM) image of the POM/MoS_2 nanocomposites (Fig. 3). Obviously, the layers of MoS_2 became thinner compared with those of the original MoS_2, which indicated that the restacked MoS_2 had good dispersion in POM. So, we affirmed that *in situ* intercalation/polymerization was a good method for preventing the agglomeration of inorganic nanoparticles.

Thermal analysis of the POM/MoS_2 nanocomposites

The thermal stabilities of pure POM and the POM/MoS_2 composite powders (without any other additives) were also studied by means of thermogravimetric analysis (TGA). Figure 4 illustrates the thermogram of pure POM and the POM/MoS_2 nanocomposite powders. A difference of the intercalated composite was the loss of weight about 10% in

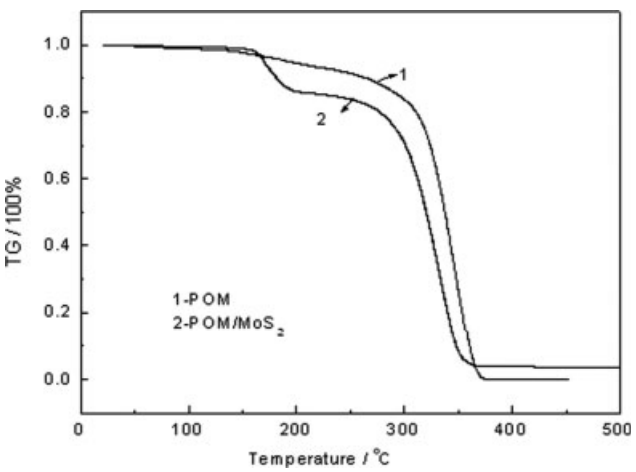

Figure 4 TGA curves of POM and POM/MoS_2.

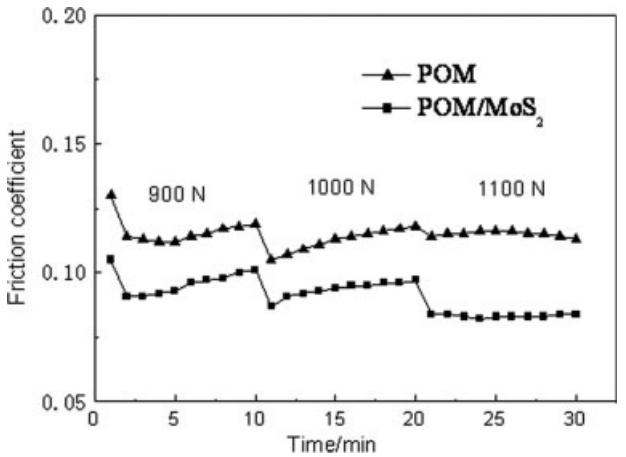

Figure 5 Relationship between the friction coefficient and load.

the range 160–220°C. It was probably related to the degradation of the lower molecular weight polymer chain. During the cationic polymerization, chain termination could take place by a reaction with MoS_2 acting as an impurity. However, the effect of intercalation on the thermal stability of the polymer was not apparent compared with the results of polyether/MoS_2 nanocomposites.[19] The difference between the temperature of maximum weight loss rate of POM and the POM/MoS_2 nanocomposites was about 10°C. The decompositions of both pure POM and the intercalated composite occurred in a relatively narrow range of temperatures.

Tribological properties of the POM/MoS_2 nanocomposites

Figure 5 represents the variation of friction coefficient with load within 30 min. These results show that the friction coefficients of the POM/MoS_2 nanocomposites were always lower than those of pure POM at different loads. That is, the POM/MoS_2 nanocomposites had better friction reduction than the pure POM. This was probably related to the thinner MoS_2 with its layered structure. The thinner MoS_2 affected the performance of the polymer matrix on a nanoscale. POM is a viscoelastic material, and its deformation under load is also viscoelastic. The friction coefficients vary with the load according to the following equation:[20]

$$\mu = k \times N^{(n-1)}$$

where μ is the coefficient of friction, N is the load, k is a constant, and n is also a constant and varies between ⅔ and 1. Thus, the coefficient of friction decreased with increasing load. The POM/MoS_2 nanocomposites exhibited better self-lubrication properties in this experiment, especially in case of higher loads. Figure 6 represents the wear scar depths of POM and the POM/MoS_2 nanocomposites. It is clear that the wear scar depth of POM/MoS_2 was smaller than that of POM, which indicates that POM/MoS_2 had better wear resistance. The MoS_2 layer could absorb the POM molecular

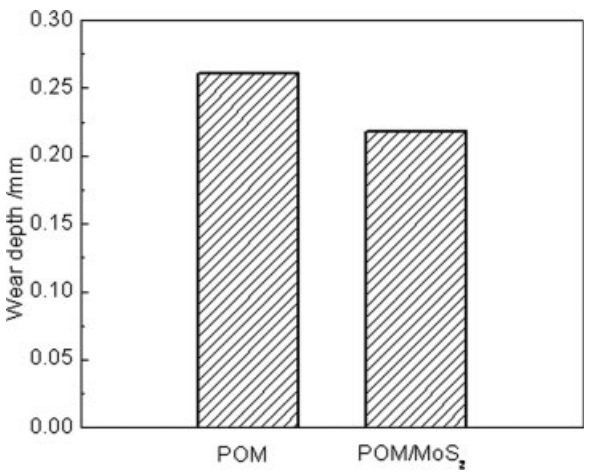

Figure 6 Comparison of the wear depths of POM and POM/MoS_2.

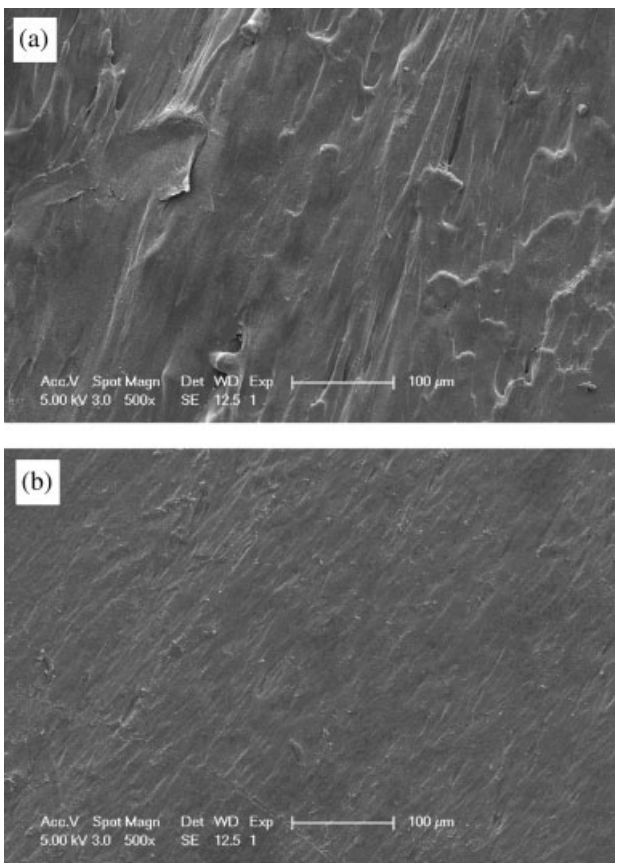

Figure 7 SEM images of (a) pure POM and (b) the POM/MoS_2 nanocomposites.

TABLE I
XPS Results for the Wear Surfaces of the POM/MoS_2 Nanocomposites

Name	Peak binding energy	Atom %
C1s	284.57	44.02
S2p	169.1	0.2
Mo3d	232.2	0.46
Fe2p	710.51	17.27
O1s	529.59	12.51
O1s	531.21	25.49
Mo3d5	228.41	0.04

segments, and this absorption could resist the plastic deformation and adhesion transfer of the POM resin.

Figure 7 shows the scanning electron microscopy (SEM) micrographs of the worn surfaces of POM and POM/MoS_2. As shown in Figure 7(a), the worn surface of POM took on a wrinkled wavy morphology surface with deep furrows in some places. This was attributed to the deformation and adhesion of the polymer. The resin melted and softened with the friction heat energy. However, the wear surface of POM/MoS_2 was smoother and could be observed only with abated scuffing, according to Figure 7(b). During the friction period, a lubrication film on the counterpart steel was seen on the macroscopic scale. It was confirmed from the results of X-ray photoelectron spectroscopy (XPS). Table I shows the XPS results of the counterpart steel surface, which rubbed against the POM/MoS_2 nanocomposites. The elements Fe, C, O, Mo, and S were detected on the rubbed surface, and the contents of C and O were very high. As show in Figure 8, the peak at 531.2 eV was well attributed to O1s of —C—O—, which was different from the 533.1-eV peak of POM and was induced by the tribological oxidization of POM. It was indicated that the lubrication film was formed on the counterpart surface by tribochemical reaction rather than physical absorption. The XPS of Fe

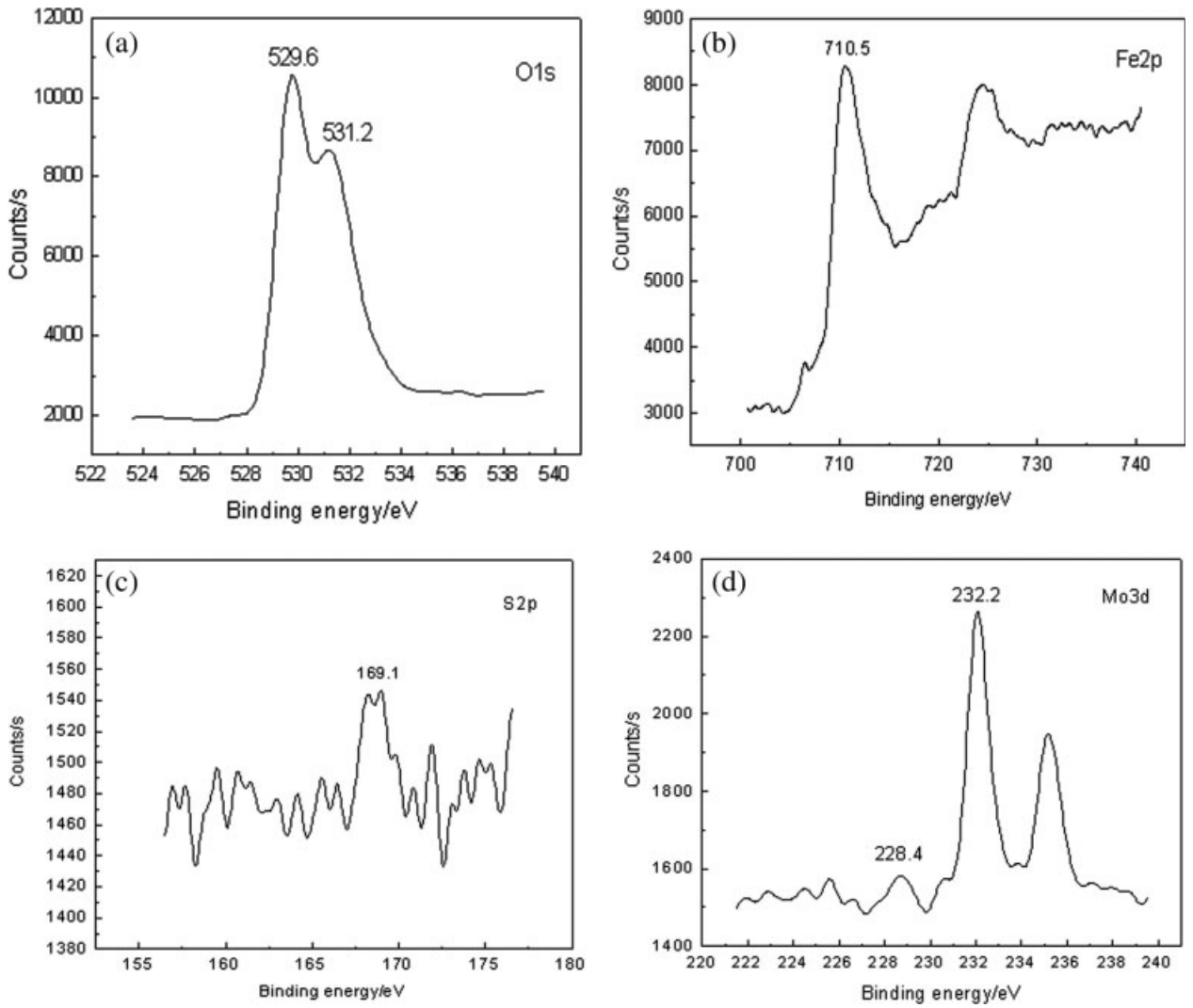

Figure 8 XPS spectra of the wear surfaces of the POM/MoS_2 nanocomposites: (a) O1s, (b) Fe2p, (c) S2p, and (d) Mo3d.

showed that the binding energy was 710.5 eV. This was ascribed to Fe2p (electrons at 2P electronic orbit of Fe) of Fe_2O_3. The two peaks at 232.2 and 228.4 eV were caused by Mo3d of MoO_3 and MoS_2, respectively. Most of Mo^{4+} was changed into Mo^{6+}, according to the XPS data. The peak at 169.1 eV corresponded to S2p (electron at 2s electronic orbit of S) of $FeSO_4$. The previous results indicate that the tribochemical reactions happened quite easily for the POM/MoS_2 nanocomposites. The lubrication film was mainly composed of alkyl chain, Fe_2O_3, and MoO_3. Also, it also had some small amounts of $FeSO_4$ and MoS_2. The resulting lubrication film could prevent continuous cutting and ploughing on the polymer surface by metal asperities.

CONCLUSIONS

POM/MoS_2 intercalated nanocomposites were synthesized successfully via *in situ* intercalation/polymerization. POM was inserted into the MoS_2 galleries, and the interlayer space expansion was 5.03 Å. The MoS_2 dispersed into the polymer matrix was still in a layer state. The heat resistance of the intercalated composites decreased slightly. The POM/MoS_2 nanocomposites exhibited better friction reduction properties than pure POM, especially under high load. The wear resistance of POM/MoS_2 was also better than that of unfilled POM. The friction mechanism was considered to be the formation of the lubrication film mainly containing alkyl chain, Fe_2O_3, and MoO_3.

References

1. Mirabal, N.; Aguirre, P.; Santa Ana, M. A.; Gonzalez, B. G. Electrochim Acta 2003, 48, 2123.
2. Fu, X.; Qutubuddin, S. Mater Lett 2000, 42, 12.
3. Wang, T. M.; Shao, X.; Wang, Q. H.; Liu, W. M. Tribology 2005, 25, 322.
4. Bissessur, R.; White, W. Mater Chem Phys 2006, 99, 214.
5. Benavente, E.; Santa Ana, M. A.; Gonzalez, G.; Becker-Guedes, F.; Mello, N. C.; Panepucci, H. C.; Bonagamba, T. J.; Donoso, J. P. Electrochim Acta 2003, 48, 1997.
6. Gonzalez, G.; Santa Ana, M. A.; Benavente, E.; Donoso, J. P.; Bonagamba, T. J.; Mello, N. C.; Panepucci, H. Solid State Ionics 1996, 85, 225.
7. Golub, A. S.; Zubavichus, Y. V.; Slovokhotov, Y. L.; Novikov, Y. N.; Danot, M. Solid State Ionics 2000, 128, 151.
8. Mirabal, N.; Lavayen, V.; Benavente, E.; Santa Ana, M. A.; Gonzalez, G. Microelectron J 2004, 35, 37.
9. Zubavichus, Y. V.; Slovokhotov, Y. L.; Schilling, P. J.; Titts-worth, R. C.; Golub, A. S.; Protzenko, G. A.; Novikov Y. N. Inorgan Chim Acta 1998, 280, 211.
10. Benavente, E.; Santa Ana, M. A.; Mendizabal, F.; Gonzalez, G. Coord Chem Rev 2002, 224, 87.
11. Zubavichus, Y. V.; Golub, A. S.; Lenenko, N. D.; Novikov, Y. N.; Slovokhotov, Y. L.; Danot, M. J Mol Catal A 2000, 158, 231.
12. Hu, X. G. Trib Lett 1998, 5, 313.
13. Wu, Y.; Hua, M. Y.; Long, C. G. Lubri Eng 2006, 6, 32.
14. Wang, H. T.; Liu, W. M.; Yang, S. R.; Xue, Q. J. Polym Mater Sci Eng 1997, 13, 126.
15. Wang, J.; Hu, X. G.; Tian, M.; Stenger, R. Polym Plast Tech Eng 2007, 46, 469.
16. Sukpirom, N.; Lerner, M. M. Mater Sci Eng A 2002, 333, 218.
17. Gee, M. A.; Frindt, R. F.; Joensen, P.; Morrison, S. R. Mater Res Bull 1986, 21, 543.
18. Yin, J. H.; Mo, Z. S. The Current Polymer Physics; Science Press: Beijing, 2001.
19. Mirabal, N.; Aguirre, P.; Santa Ana, M. A.; Benavente, E.; Gonzalez, G. Electrochim Acta 2003, 48, 2123.
20. Unal, H.; Mimaroglu, A. Mater Des 2003, 24, 183.